IOSR Journal of Applied Chemistry (IOSR-JAC)
e-ISSN: 2278-5736.Volume 10, Issue 3 Ver. I (Mar. 2017), PP 21-32
www.iosrjournals.org

Synthesis and characterization of some metal complexes of 2-Phenyl-3,4-dihydro-quinazolin-4-yloxy)-acetic acid and their Biological Application

Mostafa.A.Hussien[1,2] , W.Fathalla[3] , F. Mahmoud[3] and M.I.Megahed[3]
[1] *Department of Chemistry, Faculty of Science, Port Said University, Port Said, Egypt*
[2] *Department of Chemistry, Faculty of Science, King Abdulaziz University, Jeddah, Kingdom of saudi arabia*
[3] *Physics and Math. Engineering Dept., Faculty of Engineering, Port Said University, Port Said, Egypt*

Abstract: *2-Phenyl-3,4-dihydro-quinazolin-4-yloxy)-acetic acid (L_1) metal complexes with Mn^{2+}, Co^{2+}, Ni^{2+} Cu^{2+}, and Zn^{2+} ions were studied and the structure of the complexes were elucidated using elemental analyses, infrared (IR), ^1H nuclear magnetic resonance (NMR), magnetic moment and thermal analysis measurements. Besides the characterization of complexes by physicochemical technique,*
Biological activities of the synthesized complexes were examined against some microbial strains for evaluation of antibacterial and antifungal activities.

I. Introduction

Interest in coordination chemistry is increasing continuously with the preparation of organic ligands containing a variety of donor groups [1-3] and it is multiplied many fold when the ligands have biological importance [4,5].

Quinazolinones are one of the most important core structures present in many natural products as well as synthetic drugs. 4-(3H)-quinazolinone is frequently encountered heterocyclic moeity in medicinal chemistry known for more than a century. Quinazolinone derivatives attract a widespread interest due to the diverse biological activities [6], associated with them. They are pharmaceutically important as antituberculars [7], antibacterial [8], antiparkinsons [9], antihelmintics [10], and they also show blood platelet antiaggregatingactivity.[11]

Furthermore and taking into consideration the use of metal complexes in the treatment of some diseases, mentioned above, we described the coordination behavior of (2-Phenyl-3,4-dihydro-quinazolin-4-yloxy)-acetic acid (L_1) (Fig 1) towards some transition elements.

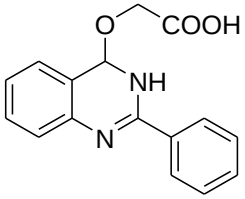

Fig.1. Structure of L_1

II. Experimental

2.1 Materials

All the compounds, solvents and nitrate salts Mn^{2+}, Co^{2+}, Ni^{2+} Cu^{2+}, and Zn^{2+} used were purchased from Aldrich and Sigma and used as received without further purification.

2.2 Instruments

Elemental analysis was carried out by standard micro chemical methods using a Perkin-Elmer CHN 2400 and the metal contents were determined gravimetrically by ignition weighted samples in air atmosphere at 1,073 K to constant weight as the metal oxide forms. The Infra-Red absorption spectrum was obtained in the solid state in the form of KBr discs and recorded using FTIR Shimadzu spectrophotometer (4000-400cm^{-1}) model 8201 DC, at the department of Chemistry, Faculty of Science, Cairo University. TG–DTG measure-ments were carried out under N_2atmosphere within the temperature range from room temperature to 1,073 K using a Shimadzu TGA-50H thermal analyzer. Electronic spectra were obtained using a Jenway 6405 Spectrophotometer with a 1 cm quartz cell. ^1H NMR spectra were measured on Bruker (300 MHz) and TMS was used as internal standard.

2.3 Preparation of (2-Phenyl-3,4-dihydro-quinazolin-4-yloxy)-acetic acid (L_1)

To a solution ester (1) (1.0 mmol) in methyl alcohol (30 ml), was added Potassium hydroxide (0.112 g, 2.0 mmol) solution in 10 ml H_2O. The reaction mixture was stirred at RT for 4 h. till complete consumption of the ester (monitored by TLC). The reaction mixture was diluted with water and acidified by Conc.HCl. The separated precipitate was filtered off and washed several times with water and dried. The resultant white product with crystalized from ethanol to give the carboxylic acid (2) in pure state. (Scheme 1)

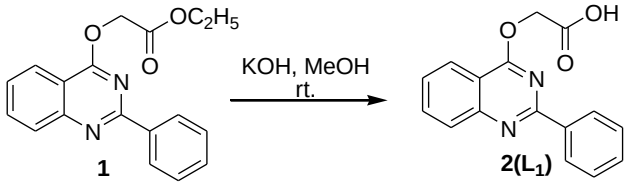

1 **2(L_1)** Scheme 1

2.4 Preparation of All complexes with ligand (L_1)

Metal complexes were prepared by dissolving (0.02 mol) of ligand (0.560 gm) in 20 ml methanol, then (0.01 mol) amounts of the metal (0.25-0.3) mg were dissolved in 10 ml methanol. The two methanolic solutions were mixed, then adjusted pH of the mixture at 8. The solution was left in air until methanol was completely evaporated. The precipitate metal complexes were filtered off, washed with acetone and drying in a desiccator. Complexes with 1:2 (M: L_1) ratios were obtained from reaction of ligand and M $(NO_3)_2$ analyses as ML_2 compound.

2.5 Antimicrobial investigation

The synthetic compounds dissolved in DMSO were tested by paper-disc agar-plate method [12], using three concentrations 30, 15 and 100 µg per disk against two reference bacterial strains (*Escherichia coli* NCMB 11943; *Staphylococcus aureus* NCMB 6571), one clinical culture (*Candida albicans*). Nutrient agar was used for testing the bacterial strains and potato dextrose agar was used for fungi. The experiment was performed in triplicate, negative controls (DMSO loaded discs) and positive controls (4 commercial antibiotic discs, Oxoid) were included. Inhibitory activity was recorded by measuring the clear zone diameter after incubation at 37°C for 24 h. for bacteria and at 30°C for 48 h. for *Candida*.

III. Results and discussion

3.1 Elemental analysis

The elemental analysis results are summarized in (Table1).These results are in good agreement with the proposed formula. The melting points of the complexes are higher than that of the free ligand, revealing that the complexes are much more stable than ligand.

Table 1: Analytical and physical data of L_1 and its metal complexes.

Compound	Formula	Yield	Found (Calc.)%				M p °C
			C	H	N	M	
L_1	**($C_{16}H_{12}N_2O_3$)**	**64**	68.57 (68.56)	32.4 (4.28)	9.99 (10)	-	180
[Mn (L_1)$_2$(H_2O)$_2$]	**($MnC_{34}H_{36}N_4O_{10}$)**	**62**	62.64 (62.65)	3.58 (3.61)	9.12 (9.14)	8.96 (8.95(	210
[Co (L_1)$_2$ (H_2O)$_2$]	**($CoC_{34}H_{36}N_4O_{10}$)**	**46**	62.23 (62.24)	3.56 (3.56)	9.08 (9.07)	9.55 (9.54)	220
[Ni (L_1)$_2$(H_2O)$_2$]	**($NiC_{34}H_{36}N_4O_{10}$).**	**58**	62.24 (62.27)	3.59 (3.56)	9.07 (9.08)	9.55 (9.51)	200
[Cu (L_1)$_2$(H_2O)$_2$]	**($CuC_{34}H_{36}N_4O_{10}$)**	**70**	61.73 (61.78)	3.53 (3.56)	9.00 (9.01)	10.22 (10.21)	195
[Zn (L_1)$_2$(H_2O)$_2$]	**($ZnC_{34}H_{36}N_4O_{10}$)**	**62**	61.64 (61.60)	3.53 (3.55)	9.00 (8.98)	10.50 (10.48)	250

3.2 Infrared spectra

The IR data for L_1 and its complexes are listed in (Table 2). The IR spectra of the complexes were compared with those of the free ligand in order to determine the coordination sites that may be involved in chelation. There are some guide peaks, in the spectra of the ligand, which are useful in achieving this goal. The position and/or the intensities of these peaks are expected to be changed upon chelation. These guide peaks are listed in

Table 2. The IR spectrum showed different signals at: 1716 (C=O acid), 1563-1577 for (COO_{asym}), 1483-1491(COOsym) and 1664-1675(C=O amideIndeed, The difference Δ(Δ = vas.COO - vs .COO) 82–94 cm^{-1} indicate bidentate metal carboxylate. From the IR spectra, it is concluded that L1 behaves as neutral bidentate ligand and binds to the metal ions through two protonated carboxylate O groups [13, 14].

Table 2: IR bands of the ligand L_1 and its complexes

Compound	ν(COO) (asymmetric)	ν(COO) (symmetric)	Δ	ν(C=O) (Acid)	ν(C=O) (Amide)	ν(M-O) (COO)	ν(M-O) (H2O)
L_1	1563	1391	172	1716	1675	--	--
[Mn $(L_1)_2(H_2O)_2$]	1566	1483	83	-	1671	430	594
[Co $(L_1)_2(H_2O)_2$]	1577	1483	94	-	1664	458	615
[Ni $(L_1)_2(H_2O)_2$]	1575	1489	86	-	1670	454	617
[Cu $(L_1)_2(H_2O)_2$]	1567	1485	82	-	1671	457	537
[Zn $(L1)_2(H_2O)_2$]	1566	1486	80	-	1672	459	538

3.3 ESR analysis

ESR spectra of powdered samples of the complexes of Cu^{2+} are similar and exhibit isotropic spectra with intense broad signals with no hyperfine structure at 300 K. The Cu^{2+}complex exhibits an axial signal with two g values (g‖ = 2.211, g⊥ = 2.049) at 300 K. In this complex, the lowest g value is >2.04 and this indicates that the copper(II) ion is present in an axial symmetry with all the principle axes aligned parallel. This would be consistent with a distorted octahedral stereochemistry (Fig.2).

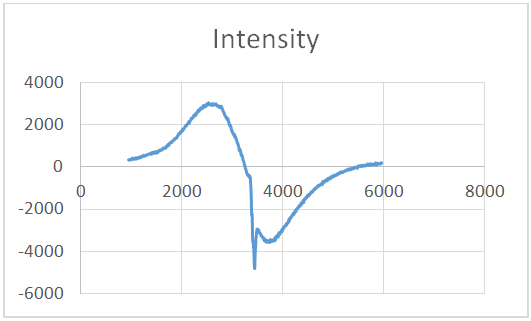

Fig.2. ESR spectra of copper (II) complexes at 300 K (A) in the solid state

3.4 NMR spectra

The structure assignment of carboxylic acid (2-phenyl-3,4-dihydro-quinazolin-4-yloxy) acetic acid (L_1) is based on ^1H and ^{13}C NMR spectroscopy , as well as physicochemical analysis, Fig. (3,4). The ^1H NMR spectrum of (L_1) in DMSO (Fig. 3) showed singlet signal at 13.22 ppm for OH group, multiplet signal between 8.50 ppm and 7.54 ppm for nine aromatic protons, singlet signal 5.24 ppm for OCH_2 group. Also, structure (L_1) was confirmed by ^{13}C NMR spectrum (Fig. 4). Signal for CO group appeared at 169.9 ppm, signals for C-Ar appeared at 166.1, 159.0, 151.8, 137.6, 135.0, 131.4, 129.1, 128.5, 128.2, 127.9, 123.7 and 114.7 ppm and signal at 63.9 ppm for OCH_2 group. (Fig. 5) shows the^{1}H-NMR spectrum
of Zn(II) complex which was carried out in DMSO-d6as a solvent. Upon comparison with the free ligand, the signal observed at 13.22 ppm can be assigned to the carboxylate OH. This signal disappears in the spectrum of the [Zn $(L1)_2$]. $2H_2O$ complex, which confirms the coordination of L_1 ligand to the M (II) ions through the deprotonated carboxylic O group.

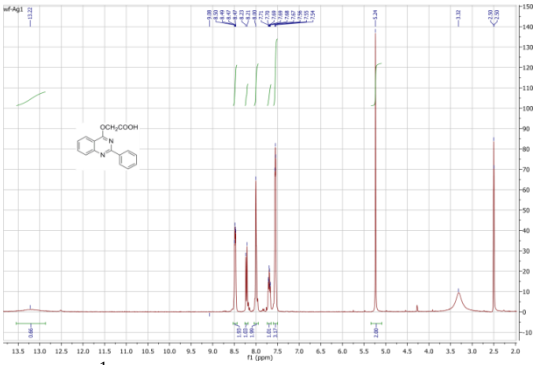

Fig 3: H^1-NMR spectrum data of the ligand (L_1)

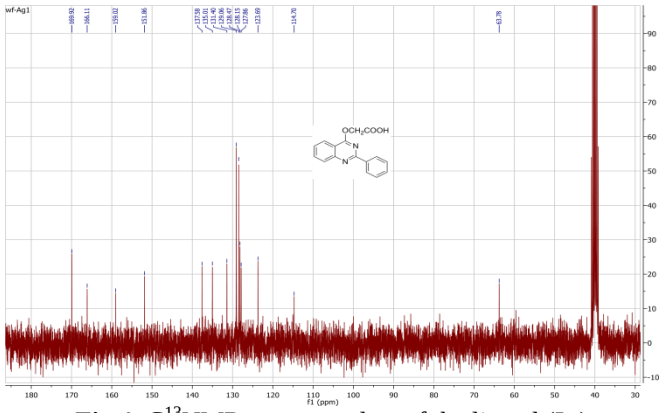

Fig 4: C^{13}NMR spectrum data of the ligand (L_1)

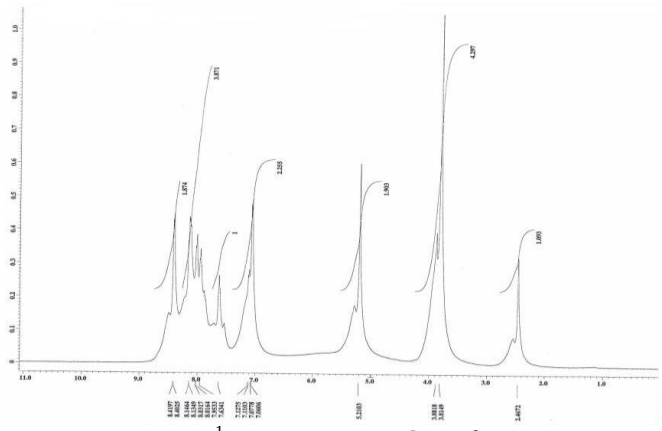

Fig 5: H^1-NMR spectrum data of ZnL_1

3.5 Thermogravimetric analysis (TG)

In the present investigation, the heating rates were controlled at 100C min^{-1} under nitrogen atmosphere and the weight loss was measured from ambient temperature up to 800C. The data are listed in (Table 4). The weight losses for each chelate were calculated within the corresponding temperature ranges. The different thermodynamic parameters are listed in (Table 5).

The thermal decomposition of ($C_{16}H_{12}N_2O_3$) (L_1) occurs at one steps. The first degradation step take place in the range of 29.22-799.07C, which assigned to loss N_2, 3(CO) and 6(C_2H_2) with the weight loss 99.1 % and the calculated value is 95.7%. The final result polluted with some carbon residue.

The thermal decomposition of **(**$MnC_{34}H_{36}N_4O_{10}$) occurs at five steps. The first degradation step take place in the range of 34.07-59.50 ^oC and it is corresponds to the eliminated of one molecule of water due to a weight loss of 2.516% in good matching with theoretical value 2.5% . The second step fall in the range of 60.03-191.32 ^oC, which assigned to loss 3(NH_3) with the weight loss 7.106% and the calculated value is 7.5%. The third step fall in the range of 192.23-333.05 ^oC, which assigned to NH_3 and 5(CO) with the weight loss 24.182% and the calculated value is 25%. The fourth step fall in the range of 333.05-441.04 ^oC, which assigned to CO_2 and 2(C_2H_2) with the weight loss 21.185% and the calculated value is 20.4%. The fifth step fall in the range of 441.04-799.49 ^oC, which assigned to 3(CH_4) and 2(C_2H_2) with the weight loss 26.780% and the calculated value is 26.67% .The 18.231% MnO is the final product remains stable till 800 ^oC polluted with some carbon atoms.

The thermal decomposition of ($CoC_{34}H_{36}N_4O_{10}$) occurs at four steps. The first degradation step take place in the range of 22.60-102.64 ^oC and it is corresponds to the eliminated of 2 molecules of water due to a weight loss of 5.079% in good matching with theoretical value 5.00% . The second step fall in the range of 103.60-336.14 ^oC, which assigned to loss 4(CO), 4(NH_3) and $CO_2$with the weight loss 32.918% and the calculated value is 32.8%. The third step fall in the range of 336.14-474.45 ^oC, which assigned to CO and 3(CH_4) with the weight loss 18.274% and the calculated value is 16.6%. The fourth step fall in the range of 475.48-799.89 ^oC, which assigned to CH_4 and 2(C_2H_2) with the weight loss 19.543% and the calculated value is 17.76% .The 24.186% CoO is the final product remains stable till 800 ^oC polluted with some carbon atoms.

The thermal decomposition of **(**$NiC_{34}H_{36}N_4O_{10}$) occurs at three steps. The first degradation step take place in the range of 29.18-100.99 ^oC and it is corresponds to the eliminated of one molecule of water due to a weight loss of 2.762% in good matching with theoretical value 2.56% . The second step fall in the range of 100.99-397.37 ^oC, which assigned to loss 5(CO), 4(NH_3), CO_2, CH_4 and 4(C_2H_2) with the weight loss 54.464%

and the calculated value is 54.4%. The third step fall in the range of 397.37-799.85 ^{o}C, which assigned to $2(C_2H_2)$ and CH_4 with the weight loss 22.756% and the calculated value is 21.9%. The 20.018% NiO is the final product remains stable till 800 ^{o}C polluted with some carbon atoms.

The thermal decomposition of ($CuC_{34}H_{36}N_4O_{10}$) **occurs** at five steps. The first degradation step take place in the range of 36.76-118.63 ^{o}C and it is corresponds to the eliminated of one molecule of water due to a weight loss of 1.832% in good matching with theoretical value 2.5% . The second step fall in the range of 119.81-201.56 ^{o}C, which assigned to loss CO with the weight loss 3.975% and the calculated value is 4.00%. The third step fall in the range of 202.49-351.86 ^{o}C, which assigned to CO, $4(NH_3)$ and CO_2 with the weight loss 21.697% and the calculated value is 21.2%. The fourth step fall in the range of 351.86-447.06 ^{o}C, which assigned to CO_2 and CO with the weight loss 12.646% and the calculated value is 13.58%. The fifth step fall in the range of 448.05-799.84 ^{o}C, which assigned to $3(CH_4)$ and $4(C_2H_2)$ with the weight loss 32.91% and the calculated value is 33.9% .The 26.94% CuO is the final product remains stable till 800 ^{o}C and 18 unoxidized carbon atoms.

The thermal decomposition of ($ZnC_{34}H_{36}N_4O_{10}$) occurs at five steps. The first degradation step take place in the range of 43.43-108.53 ^{o}C and it is corresponds to the eliminated of half molecule of water due to a weight loss of 1.199% in good matching with theoretical value 1.29% . The second step fall in the range of 109.18-308.26 ^{o}C, which assigned to loss $4(NH_3)$ and CO_2 with the weight loss 16.679% and the calculated value is 16.24%. The third step fall in the range of 308.26-377.30 ^{o}C, which assigned to 2CO with the weight loss 10.916% and the calculated value is 9.79%. The fourth step fall in the range of 377.30-548.84 ^{o}C, which assigned to CO_2 and CO with the weight loss 14.598% and the calculated value is 13.9%. The fifth step fall in the range of 549.01-799.91 ^{o}C, which assigned to $4(CH_4)$ and $2(C_2H_2)$ with the weight loss 28.829% and the calculated value is 26.7% .The 27.779% ZnO is the final product remains stable till 800 ^{o}C and 21 unoxidized carbon atoms. Reported data dealing in the thermal analysis investigation within nitrogen atmosphere indicate that, the Zn(II) complex decompose to give oxide contaminated with few carbon atoms as final products, this reason because of no sufficiently of oxygen atoms help to evolved carbon as carbon monoxide or dioxide.

The different thermodynamic parameters were calculated upon Coats-Redfern [15] and Horowitz-Metzger [16] methods and listed in Table 4. The activation energies of decomposition found to be in the range 1.00 $x10^5$ - 9.58 $x10^4$ $kJmol^{-1}$. The high values of the activation energies reflect the thermal stability of the complexes. The entropy of activation found to have negative values in all the complexes, which indicate that the decomposition reactions proceed with a lower rate than the normal ones. On another meaning the thermal decomposition process of all complexes are non-spontaneous, i.e, the complexes are thermally stable. The correlation coefficients of the Arhenius plots of the thermal decomposition steps found to lie in the range 0.7758 to 0.9963, showing a good fit with linear function.

Table 4 : Thermodynamic data of the thermal decomposition of ligand (L_1) and its complexes

Comp.[a]	TG range (C)	DTA (C)	Stage	Mass loss %found(calc.)	Assignment	Metallic residue
L_1 ($C_{16}H_{12}N_2O_3$)	29.22-799.07	414.145	1st	99.1 (95.7)	N_2,3(CO), $6(C_2H_2)$	Carbon residue
[Mn $(L_1)_2(H_2O)_2$]	34.07-59.50	47.2897	1st	2.516 (2.5)	H_2O	MnO
	60.03-191.32	120.124	2nd	7.106 (7.5)	$3(NH_3)$	
	192.23-333.05	266.893	3rd	24.182 (25)	NH_3, 5(CO)	
	333.05-441.04	381.255	4th	21.185 (20.4)	CO_2, $2(C_2H_2)$	
	441.04-799.49	604.322	5th	26.780 (26.67)	$3(CH_4)$,$2(C_2H_2)$	
[Co $(L_1)_2(H_2O)_2$]	22.60-102.64	64.666	1st	5.079 (5.00)	$2H_2O$	CoO
	103.60-336.14	270.7	2nd	32.918 (32.8)	$4(CO)$,$4(NH_3)$, CO_2	
	336.14-474.45	428.09	3rd	18.274 (16.6)	CO , $3(CH_4)$	
	475.48-799.89	637.685	4th	19.543 (17.76)	CH_4, $2(C_2H_2)$	
[Ni $(L_1)_2(H_2O)_2$]	29.18-100.99	67.1966	1st	2.762 (2.56)	H_2O	NiO
	100.99-397.37	271.614	2nd	54.464 (54.4)	5(CO),$4(NH_3)$, CO_2, CH_4, $4(C_2H_2)$	
	397.37-799.85	598.61	3rd	22.756 (21.9)	$2(C_2H_2)$, CH_4	
[Cu $(L_1)_2(H_2O)_2$]	36.76-118.63	86.5487	1st	1.832 (2.5)	H_2O	CuO
	119.81-201.56	169.376	2nd	3.975 (4.00)	CO	
	202.49-351.86	283.16	3rd	21.697 (21.2)	CO, $4(NH_3)$, CO_2	
	351.86-447.06	400.473	4th	12.646 (13.58)	CO, CO_2	
	448.05-799.84	623.945	5th	32.91 (33.9)	$3(CH_4)$,$4(C_2H_2)$	
[Zn $(L_1)_2(H_2O)_2$]	43.43-108.53	82.7016	1st	1.199 (1.29)	0.5 (H_2O)	ZnO
	109.18-308.26	256.178	2nd	16.679 (16.24)	$4(NH_3)$, CO_2	
	308.26-377.30	346.404	3rd	10.916 (9.79)	2 (CO)	
	377.30-548.84	463.07	4th	14.598 (13.9)	CO, CO_2	
	549.01-799.91	675.774	5th	28.829 (26.7)	$4(CH_4)$,$2(C_2H_2)$	

Table 5 : Thermodynamic data of the thermal decomposition of ligand (L_1) and its complexes

	Stage	Method	E	A	-ΔS	ΔH	ΔG	R
$[Mn(L_1)_2(H_2O)_2]$	1st	CR	1.48E+05	3.09E+03	1.79E+02	1.45E+05	2.02E+05	0.97374
		HM	1.54E+04	9.94E-01	2.46E+02	1.28E+04	9.15E+04	0.9785
		Average	8.16E+04	1.55E+03	2.12E+02	7.89E+04	1.47E+05	0.97612
	2nd	CR	2.03E+04	3.99E+00	2.36E+02	1.70E+04	1.10E+05	0.93397
		HM	3.56E+04	2.47E+02	2.01E+02	3.23E+04	1.12E+05	0.9449
		Average	2.79E+04	1.25E+02	2.19E+02	2.47E+04	1.11E+05	0.939435
	3th	CR	8.20E+04	1.85E+05	1.49E+02	7.75E+04	1.58E+05	0.99185
		HM	9.58E+04	1.21E+07	1.14E+02	9.13E+04	1.53E+05	0.99798
		Average	8.89E+04	6.13E+06	1.32E+02	8.44E+04	1.55E+05	0.994915
	4th	CR	1.21E+05	1.64E+07	1.13E+02	1.16E+05	1.90E+05	0.96821
		HM	1.34E+05	3.26E+08	8.85E+01	1.29E+05	1.87E+05	0.96041
		Average	1.28E+05	1.71E+08	1.01E+02	1.22E+05	1.88E+05	0.96431
	5th	CR	4.04E+04	2.72E-01	2.65E+02	3.31E+04	2.65E+05	0.63789
		HM	5.62E+04	3.23E+00	2.44E+02	4.89E+04	2.63E+05	0.72114
		Average	4.83E+04	1.75E+00	2.54E+02	4.10E+04	2.64E+05	0.679515
$[Co(L_1)_2(H_2O)_2]$	1st	CR	6.19E+04	3.24E+07	1.02E+02	5.91E+04	9.36E+04	0.9731
		HM	6.77E+04	3.52E+08	8.23E+01	6.49E+04	9.27E+04	0.95985
		Average	6.48E+04	1.92E+08	9.23E+01	6.20E+04	9.32E+04	0.966475
	2nd	CR	3.80E+04	1.42E+03	1.90E+02	3.34E+04	1.37E+05	0.94339
		HM	1.15E+05	9.45E+08	7.81E+01	1.11E+05	1.53E+05	0.95189
		Average	7.67E+04	4.72E+08	1.34E+02	7.22E+04	1.45E+05	0.94764
	3th	CR	1.12E+05	5.41E+05	1.42E+02	1.06E+05	2.06E+05	0.86684
		HM	1.32E+05	3.78E+07	1.07E+02	1.26E+05	2.01E+05	0.91022
		Average	1.22E+05	1.92E+07	1.25E+02	1.16E+05	2.03E+05	0.88853
	4th	CR	1.06E+05	5.14E+03	1.83E+02	9.88E+04	2.55E+05	0.95498
		HM	1.22E+05	9.50E+04	1.58E+02	1.15E+05	2.50E+05	0.94567
		Average	1.14E+05	5.01E+04	1.70E+02	1.07E+05	2.52E+05	0.950325
	5th	CR	2.35E+05	6.52E+09	6.72E+01	2.26E+05	2.94E+05	0.97166
		HM	2.50E+05	3.90E+10	5.23E+01	2.42E+05	2.95E+05	0.97551
		Average	2.43E+05	2.27E+10	5.98E+01	2.34E+05	2.95E+05	0.973585

[Ni $(L_1)_2(H_2O)_2$]	**1st**	CR	4.84E+04	1.19E+05	1.49E+02	4.56E+04	9.62E+04	0.9963
		HM	5.56E+04	3.32E+06	1.21E+02	5.28E+04	9.40E+04	0.9948
		Average	5.20E+04	1.72E+06	1.35E+02	4.92E+04	9.51E+04	0.99555
	2nd	CR	4.32E+04	1.00E+04	1.73E+02	3.87E+04	1.33E+05	0.9889
		HM	1.30E+05	2.71E+10	5.02E+01	1.26E+05	1.53E+05	0.99489
		Average	8.67E+04	1.35E+10	1.12E+02	8.22E+04	1.43E+05	0.991895
	3th	CR	2.06E+05	7.22E+09	6.48E+01	1.99E+05	2.53E+05	0.82911
		HM	2.22E+05	4.58E+11	3.03E+01	2.15E+05	2.40E+05	0.77588
		Average	2.14E+05	2.32E+11	4.75E+01	2.07E+05	2.46E+05	0.80247
	4th	CR	1.22E+05	6.85E+03	1.82E+02	1.13E+05	3.01E+05	0.85958
		HM	1.41E+05	3.70E+04	1.68E+02	1.33E+05	3.06E+05	0.90153
		Average	1.31E+05	2.19E+04	1.75E+02	1.23E+05	3.04E+05	0.880555
[Cu $(L_1)_2(H_2O)_2$]	**1st**	CR	4.63E+04	4.67E+04	1.57E+02	4.33E+04	9.98E+04	0.93374
		HM	5.29E+04	3.93E+05	1.39E+02	4.99E+04	1.00E+05	0.93608
		Average	4.96E+04	2.20E+05	1.48E+02	4.66E+04	9.99E+04	0.93491
	2nd	CR	2.43E+04	1.86E+01	2.24E+02	2.06E+04	1.20E+05	0.98145
		HM	5.24E+04	8.18E+03	1.73E+02	4.87E+04	1.25E+05	0.98318
		Average	3.83E+04	4.10E+03	1.99E+02	3.47E+04	1.23E+05	0.982315
	3th	CR	1.00E+05	8.30E+06	1.18E+02	9.54E+04	1.61E+05	0.96364
		HM	1.13E+05	3.11E+08	8.75E+01	1.09E+05	1.57E+05	0.94203
		Average	1.07E+05	1.60E+08	1.03E+02	1.02E+05	1.59E+05	0.952835
	4th	CR	1.66E+05	4.04E+10	4.86E+01	1.61E+05	1.93E+05	0.99078
		HM	1.80E+05	6.59E+11	2.54E+01	1.74E+05	1.91E+05	0.98585
		Average	1.73E+05	3.50E+11	3.70E+01	1.67E+05	1.92E+05	0.988315
	5th	CR	8.66E+04	2.56E+02	2.07E+02	7.96E+04	2.55E+05	0.95811
		HM	1.04E+05	6.97E+03	1.80E+02	9.65E+04	2.49E+05	0.95148
		Average	9.51E+04	3.61E+03	1.94E+02	8.80E+04	2.52E+05	0.954795
	6th	CR	3.80E+05	7.85E+03	1.81E+02	3.72E+05	5.57E+05	0.98296
		HM	4.01E+04	8.37E-02	2.76E+02	3.16E+04	3.15E+05	0.98156
		Average	2.10E+05	3.93E+03	2.28E+02	2.02E+05	4.36E+05	0.98226

$[Zn(L_1)_2(H_2O)_2]$	1st	CR	4.06E+04	9.92E+03	1.70E+02	3.77E+04	9.81E+04	0.78797
		HM	4.69E+04	5.63E+04	1.55E+02	4.39E+04	9.92E+04	0.82963
		Average	4.37E+04	3.31E+04	1.63E+02	4.08E+04	9.87E+04	0.8088
	2nd	CR	2.78E+04	3.74E+01	2.20E+02	2.34E+04	1.40E+05	0.94431
		HM	8.35E+04	1.03E+06	1.35E+02	7.91E+04	1.50E+05	0.94823
		Average	5.57E+04	5.16E+05	1.77E+02	5.12E+04	1.45E+05	0.94627
	3th	CR	2.04E+05	4.20E+03	1.82E+02	1.99E+05	3.11E+05	0.93393
		HM	2.18E+04	7.81E-02	2.72E+02	1.66E+04	1.85E+05	0.92565
		Average	1.13E+05	2.10E+03	2.27E+02	1.08E+05	2.48E+05	0.92979
	4th	CR	2.02E+05	1.04E+13	2.64E+00	1.96E+05	1.98E+05	0.96257
		HM	2.12E+04	3.74E-02	2.79E+02	1.55E+04	2.07E+05	0.95891
		Average	1.12E+05	5.20E+12	1.41E+02	1.06E+05	2.02E+05	0.96074
	5th	CR	1.71E+05	1.03E+09	8.03E+01	1.64E+05	2.27E+05	0.93871
		HM	1.82E+05	1.13E+10	6.04E+01	1.76E+05	2.23E+05	0.93789
		Average	1.76E+05	6.18E+09	7.04E+01	1.70E+05	2.25E+05	0.9383
	6th	CR	1.25E+05	9.34E+03	1.79E+02	1.17E+05	2.87E+05	0.97453
		HM	1.44E+05	2.76E+05	1.50E+02	1.36E+05	2.79E+05	0.9624
		Average	1.35E+05	1.43E+05	1.64E+02	1.27E+05	2.83E+05	0.968465

3.6 Molecular structure

The selected geometrical structure of the investigated ligand is calculated by optimizing their bond length and bond angles (Table 6). The highest occupied molecular orbital (HOMO) and lowest unoccupied molecular orbital (LUMO) energy gaps in Fig.6 , ΔE, which is an important stability index, applied to develop theoretical models for explaining the structure and conformation in many molecular systems. The smaller is the value of ΔE, the more is the reactivity of the compound has the calculated quantum chemical parameters are given in (Table 7).

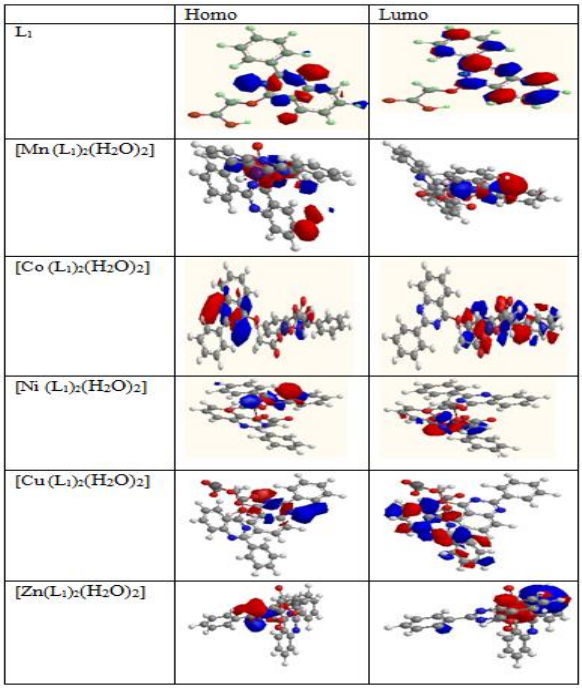

Fig. 6. The molecular structure of L_1 and its complexes

Table 6: The calculated quantum chemical parameters for $L_1$and its complexes.

Comp	E_{HUMO} eV	E_{LUMO} eV	ΔE eV	X eV	η eV	δ eV	Pi eV	σ eV	S eV	Ω eV	ΔN max
L_1	-7.034	-3.342	3.692	5.188	1.846	0.54171181	-5.188	0.541711	0.923	7.290179	2.8104
$[Mn(L_1)_2(H_2O)_2]$	-8.869	-7.035	1.834	7.952	0.917	1.09051254	-7.952	0.4585	0.4585	3.976	8.6717
$[Co(L_1)_2(H_2O)_2]$	-7.032	-3.345	3.687	5.1885	1.8435	0.54244643	-5.1885	0.92175	0.92175	2.59425	2.8144
$[Ni(L_1)_2(H_2O)_2]$	-7.089	-7.042	0.047	7.0655	0.0235	42.5531915	-7.0655	0.01175	0.01175	3.53275	300.65
$[Cu(L_1)_2(H_2O)_2]$	-7.055	-3.356	3.699	5.2055	1.8495	0.54068667	-5.2055	0.92475	0.92475	2.60275	2.8145
$[Zn(L_1)_2(H_2O)_2]$	-7.040	-3.52	3.52	5.28	1.76	0.56818182	-5.28	0.88	0.88	2.64	3

Table 7: Bond length and Bond angels of ligand

Bond length		**Bond angle**	
L_1			
O(21)-H(33)	0.971	H(33)-O(21)-C(19)	111.651
C(19)-O(21)	1.352	O(21)-C(19)-O(20)	124.710
C(19)-O(20)	1.212	O(21)-C(19)-C(18)	110.441
C(18)-H(32)	1.115	O(20)-C(19)-C(18)	124.844
C(18)-H(31)	1.114	H(32)-C(18)-H(31)	109.784
C(18)-C(19)	1.523	H(32)-C(18)-C(19)	107.640
O(17)-C(18)	1.413	H(32)-C(18)-O(17)	109.521
C(16)-H(30)	1.103	H(31)-C(18)-C(19)	109.850
C(15)-H(29)	1.103	H(31)-C(18)-O(17)	109.441
C(15)-C(16)	1.343	C(19)-C(18)-O(17)	110.582
C(14)-H(28)	1.103	C(18)-O(17)-C(10)	116.244
C(14)-C(15)	1.340	H(30)-C(16)-C(15)	115.907
C(13)-H(27)	1.103	H(30)-C(16)-C(11)	121.941
C(13)-C(14)	1.340	C(15)-C(16)-C(11)	122.152
C(12)-H(26)	1.103	H(29)-C(15)-C(16)	120.157
C(12)-C(13)	1.343	H(29)-C(15)-C(14)	119.593
C(11)-C(16)	1.351	C(16)-C(15)-C(14)	120.249
C(11)-C(12)	1.351	H(28)-C(14)-C(15)	120.536
C(10)-O(17)	1.372	H(28)-C(14)-C(13)	120.534
N(9)-C(10)	1.267	C(15)-C(14)-C(13)	118.930
C(8)-C(11)	1.357	H(27)-C(13)-C(14)	119.596
C(8)-N(9)	1.270	H(27)-C(13)-C(12)	120.155
N(7)-C(8)	1.270	C(14)-C(13)-C(12)	120.249
C(6)-H(25)	1.103	H(26)-C(12)-C(13)	115.871
C(10)-C(5)	1.345	H(26)-C(12)-C(11)	121.979
C(5)-C(6)	1.345	C(13)-C(12)-C(11)	122.150
C(4)-N(7)	1.265	C(16)-C(11)-C(12)	116.269
C(4)-C(5)	1.344	C(16)-C(11)-C(8)	121.868
C(3)-H(24)	1.104	C(12)-C(11)-C(8)	121.862
C(3)-C(4)	1.345	O(17)-C(10)-N(9)	117.756
C(2)-H(23)	1.103	O(17)-C(10)-C(5)	123.363
C(2)-C(3)	1.342	N(9)-C(10)-C(5)	118.874
C(1)-H(22)	1.103	C(10)-N(9)-C(8)	122.488
C(6)-C(1)	1.342	C(11)-C(8)-N(9)	119.759
C(2)-C(1)	1.341	C(11)-C(8)-N(7)	119.960
		N(9)-C(8)-N(7)	120.280
		C(8)-N(7)-C(4)	121.303
		H(25)-C(6)-C(5)	121.452
		H(25)-C(6)-C(1)	118.281
		C(5)-C(6)-C(1)	120.267
		C(10)-C(5)-C(6)	123.350
		C(10)-C(5)-C(4)	116.937
		C(6)-C(5)-C(4)	119.714
		N(7)-C(4)-C(5)	120.117
		N(7)-C(4)-C(3)	120.040
		C(5)-C(4)-C(3)	119.843
		H(24)-C(3)-C(4)	120.475
		H(24)-C(3)-C(2)	119.194
		C(4)-C(3)-C(2)	120.332
		H(23)-C(2)-C(3)	120.121
		H(23)-C(2)-C(1)	120.058
		C(3)-C(2)-C(1)	119.822
		H(22)-C(1)-C(6)	120.084
		H(22)-C(1)-C(2)	119.894

		C(6)-C(1)-C(2)	120.022
Mn L_1			
Mn(41)-O(43)	1.813	Mn(41)-O(43)-C(19)	115.788
Mn(41)-O(40)	1.813	O(43)-Mn(41)-O(40)	91.640
		Mn(41)-O(40)-C(38)	116.193
Co L_1			
Co(41)-O(43)	0.772	O(43)-Co(41)-O(40)	119.827
Co(41)-O(40)	0.768	Co(41)-O(40)-C(38)	120.131
Ni L_1			
Ni(41)-O(43)	1.790	Ni(41)-O(43)-C(19)	112.868
Ni(41)-O(40)	1.791	O(43)-Ni(41)-O(40)	91.892
		Ni(41)-O(40)-C(38)	108.604
Cu L_1			
Cu(41)-O(40)	1.811	Cu(41)-O(43)-C(19)	114.331
		O(43)-Cu(41)-O(40)	110.226
		Cu(41)-O(40)-C(38)	112.668
Zn L_1			
Zn(41)-O(43)	1.891	Zn(41)-O(43)-C(19)	112.122
Zn(41)-O(40)	1.891	O(43)-Zn(41)-O(40)	119.660
		Zn(41)-O(40)-C(38)	112.052

3.7 Molecular docking

Cancer can be described as the uncontrolled growth of abnormal cells. Breast cancer is one of the most recurring worldwide diagnosed and deadliest cancers next to lung cancer with a high number of mortality rates among females [17]. At global level, it accounted for more than 1.6 million new cases in 2010. The incidence or prevalence rate of the breast cancer in India is expected to be more than 90,000 in the coming years and over 50,000 women die each year.

Docking study showed the binding affinity, number of hydrogen bonds. It is interesting to note that the binding affinities have negative values. This reveals the high feasibility of this reaction. Molecular docking is a key tool in computer drug design [18, 19]. The focus of molecular docking is to simulate the molecular recognition process. Molecular docking aims to achieve an optimized conformation for both the protein and drug with relative orientation between them such that the free energy of the overall system is minimized. The docked ligand were analysis breast Cancer 3hb5 as shown in Fig. 7.

The study simulates the actual docking process in which the ligand – protein pair-wise interaction energies are calculated using Docking Server [20] in (Table 8). According to our results, HB plot curve indicate that, compound binds to the two protein with hydrogen bond interactions of ligands (L1) with 3hb5 as shown in Fig 8. The calculated efficiency is favorable, Ki values estimated by Auto Dock were compared with experimental Ki values, when available, and the Gibbs free energy is negative. Also, based on this data, we can propose that interaction between, 3hb5 receptors and the ligands (L1) is possible. 2D plot curve of docking with ligands (L1) are shown in Fig 8. This interaction could activate apoptosis in cancer cells energy of interactions with ligand (L1). From the analysis of the values, it is evident that the binding energy of (L1) is higher value increased of binding affinity ligand towards the receptor. The characteristic feature of ligand represent in presence of several active sites available for hydrogen bonding. This feature gives them the ability to be good binding inhibitors to the protein and will help to produce augmented inhibitory compounds. The results confirm that, ligand is efficient inhibitor of 3hb5–oxidorductase breast cancer.

Table.8: Energy values obtained in docking calculations of ligand (L_1) with receptor breast cancer 3hb5

Comp	Est. Free Energy of Binding	Est. Inhibition Constant, Ki	vdW + Hbond + desolv Energy	Electrostatic Energy	Total Intermolec. Energy	Interact. Surface
L_1	-6.91 kcal/mol	8.64 uM	-7.98 kcal/mol	-0.09 kcal/mol	-8.08 kcal/mol	717.445

Fig. 7. The ligand (L_1) (green in (1A) and blue in (1B) in interaction with receptor breast cancer (3hb5**)**

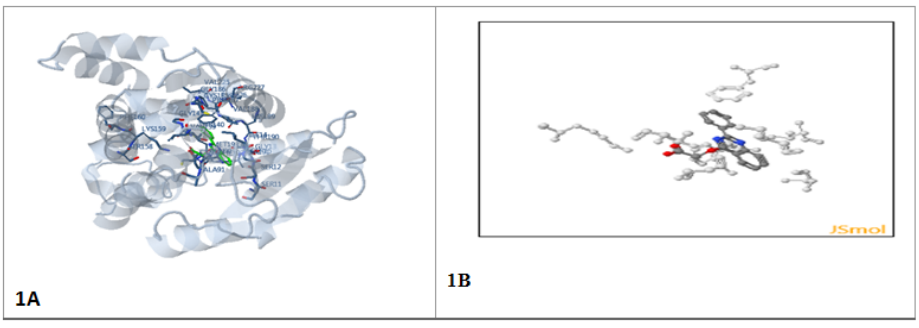

Fig. 8. 2D plot of interaction between the ligand (L_1) and receptor breast cancer 3hb5

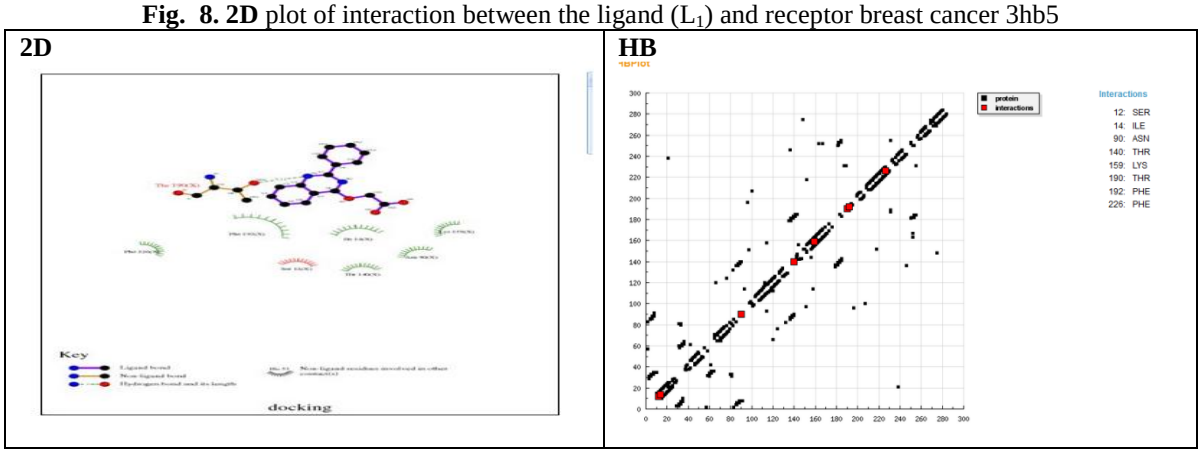

3.8 Microbiological investigation

The last part of this study investigate the antimicrobial activities of the synthesized compounds against Gram-positive bacteria Staphylococcus aureus, Gram-negative bacteria *Escherichia coli* and (Candida albicans). The antimicrobial activity was expressed by the inhibition zone. The results as shown in (table 8) showed that complexes exhibited good activity, whereas the Cu(II)and Zn(II) complexes are more active than the Ni(II), Mn(II) and Co(II) complexes against Gram-positive bacteria Staphylococcus aureus, Gram-negative bacteria *Escher-ichia coli* and (Candida albicans) greater than the standard drugs (Tetracycline, Novobiocin, Erythromycin and Neomycin).

Table.9: Antimicrobial analysis of ligand (L_1) and its complexes

Antibacterial Activity			**Antifungal Activity**
Zone Of Inhibition (mm)			**Zone Of Inhibition (mm)**
Code No.	***Escherichia coli***	***Staphylococcus aureus***	***Candida albicans***
Samples (30 □l each) were analyzed using "disc diffusion method"			
Control	-ve	-ve	-ve
MnL_1	0.8	-ve	0.9
CoL_1	1.1	2.2	1.8
NiL_1	1.3	2.0	2.3
CuL_1	2.5	2.7	2.3
ZnL_1	1.7	2.3	1.7
(L_1)	1.7	2.0	1.8
Tetracycline	0.7	0.6	1.2
Novobiocin	-ve	-ve	2
Samples (15 □l each) were analyzed using "disc diffusion method"			
Control	-ve	-ve	-ve
ZnL_1	1.5	1.7	1.7
CuL_1	2.3	2.4	2.6
(L_1)	1.7	1.4	1.1
Erythromycin	-ve	-ve	2
Samples (10 □l each) were analyzed using "disc diffusion method"			
Control	-ve	-ve	-ve
CuL_1	1.8	2.0	2.7
Neomycin	1	1.2	1.1

IV. Conclusion

New Octahedral complexes of Mn(II), Co(II), Ni(II), Cu(II) and Zn(II) with (2-Phenyl-3,4-dihydro-quinazolin-4-yloxy)-acetic acid (L_1) have synthesized and characterized using infrared, electronic and thermal. The ligand has been found to act as bidentate chelating agent. L_1 complexes coordinate through the carboxyl group with 1:2 molar ratio as shown in Fig 9. Antibacterial screening of the complexes against Escherichia Coli, Staphylococcus aureus and antifungal (Candida albicans activities) was also investigated. The metal complexes were found to have varied degree of inhibitory effect against the bacteria and fungi greater than the standard drugs (Tetracycline, Novobiocin, Erythromycin and Neaomycin).

M= Co (II), Ni (II), Mn (II), Cu(II) and Zn(II)
Fig.9. Proposed structure of the metal complexes

References

[1]. Hancock RD, Martell AE (1989). Ligand design for selective complexation of metal ions in aqueous solution. Chem. Rev. 9: 1875-1914.
[2]. Bhyrappa P, Young JK, Moore JS, Suslick KS (1996). DendrimerMetalloporphyrins: Synthesis and Catalysis. J. Am. Chem. Soc. 118:5708-5711.
[3]. Castillo-Blum SE, Barba-Behrens N (2000). Coordination chemistry of some biologically active ligands. Coord. Chem. Rev. 196: 3-30.
[4]. Mohan G, Rajesh N (1992). Synthesis and anti-inflammatory activity of N-pyridinobenzamide-2-carboxylic acid and its metal chelates. IndianJ. Pharm. 24: 207-211.
[5]. Kong D, Reibenspies J, Mao J, Clearfield A (2003). Novel 30-membered octaazamacrocyclic ligand: synthesis, characterization, thermodynamic stabilities and DNA cleavage activity of homodinuclear copper and nickel complexes. Inorg. Chim. Acta 342: 158-170.
[6]. V. Joshi, R. P. Chaudhari, Indian J Chem.26B, 602 (1987).
[7]. VK. Srivastava, SS. Gulati, K. Shanker, Indian J Chem., 26B, 652 (1987).
[8]. DP. Gupta, S. Ahmad, A. Kumar, K. Shanker, Indian J Chem, 27B, 1060 (1988).
[9]. K. Sakai, H. Nahata, J. Jpn Kokai Tokyo Koho JP. 329, 6351 (1988).
[10]. V. Niementowski, J. Prakt Chem., 51, 564 (1895).
[11]. SN. Pandeya, D. Sriram, G. Nath, E D Clercq., J.Pharm. Acta Helvetiae. 74, 17 (1999).
[12]. E. J. De Beer, M. B. Sherwood, J. Bacteriol, 4, 459 (1945).
[13]. M.S. Refat, S.A. El-Korashy, M.A. Hussien, Canadian Chemical Transactions 2 (1), 97-107, 2014
[14]. M.S. Refat, S.A .El-Korashy, M.A. Hussien, Canadian Chemical Transactions 2 (1), 24-35, 2014
[15]. Coats, A.W.; Redfern, J.P. Kinetic Parameters from Thermogravimetric Data. Nature 1964, 201, 68- 69.
[16]. Horowitz, H.H.; Metzger, G. A new analysis of thermogravimetric traces. Anal. Chem. 1963, 35, 1464- 1468.
[17]. Bikadi, Z., Hazai, E. Application of the PM6 semi-empirical method to modeling proteins enhances docking accuracy of AutoDockJ. Cheminf. 1, 15 (2009)
[18]. T. A. Halgren Merck molecular force field. I. Basis, form, scope, parametrization, and performance of MMFF94 Journal of Computational Chemistry 17 (5-6), 490-519 (1998)
[19]. G. M. Morris, D. S. Goodsell, et al. Automated docking using a Lamarckian genetic algorithm and an empirical binding free energy function Journal of Computational Chemistry 19 (14), 1639-1662 (1998)
[20]. F. J. Solis and R. J. B. Wets Minimization by Random Search Techniques Mathematics of Operations Research 6 (1), 19-30 (1981)